ACS Catalysis

RESEARCH ARTICLE

pubs.acs.org/acscatalysis

# What Makes for a Bad Catalytic Cycle? A Theoretical Study on the Suzuki−Miyaura Reaction within the Energetic Span Model

Sebastian Kozuch*,† and Jan M. L. Martin‡

†Department of Organic Chemistry, Weizmann Institute of Science, IL-76100 Rechovot, Israel

‡Department of Chemistry and the Center for Advanced Scientific Computing and Modeling (CASCAM), University of North Texas, Denton, Texas 76203-5017, United States

Supporting Information

**ABSTRACT:** The Suzuki−Miyaura cross-coupling reaction using $PMe_3$, $PPh_3$, and $PtBu_3$ as ligands was studied theoretically with accurate density functional theory (DFT) methods and the Energetic Span Model. The energetic span model is a tool to compute catalytic turnover frequencies (TOF) from computationally obtained energy states. In this work the model is expanded to include turnover numbers (TON) and off-cycle intermediates. The results show that although the monophosphine route is the fastest pathway, the diphosphine cis route (accessible for small ligands) may also be reactive. The death sentence of the $PMe_3$ catalyst is the possibility to reach the low energy trans diphosphine species, which substantially reduces the TON. In the $PPh_3$ case, the formation of $Pd^0L_3$ was found to be the major drawback for efficient catalysis. The $PtBu_3$ system is the most efficient of the three, as only the monophosphine mechanism is accessible.

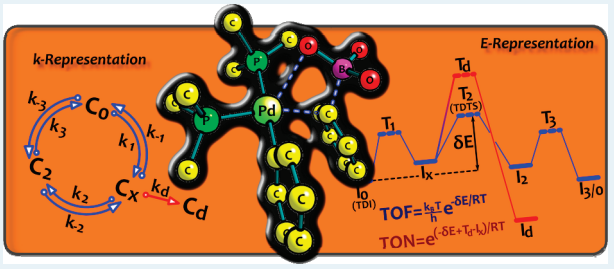


**KEYWORDS:** energetic span, cross-coupling, Suzuki−Miyaura, theoretical, density functional theory

## INTRODUCTION: SUZUKI−MIYAURA REACTION

The cross-coupling reaction of Suzuki−Miyaura has proven to be a practical way to generate C−C bonds by coupling an organic halide with an organoboron molecule, in the presence of a palladium catalyst (see Figure 1).[1−7] The reaction proceeds in a basic medium, thus a boronate is the substrate involved in the substitution of the halide from the $Pd^{II}$ complex.[8,9]

It is known that bulky phosphines with big cone angles[10] like $PtBu_3$[11,12] are more effective than small phosphines for cross-coupling reactions.[1−3,13−17] The size of the ligand is even more important than its electronic effects,[18,19] since while the electron donating/withdrawing power of the ligand can "fine-tune" the oxidative addition and reductive elimination steps,[1−3] a bulky ligand will qualitatively change the mechanism of the reaction by forcing the dissociation of a phosphine. The monophosphine pathway produced by bulky ligands is a constant factor in highly efficient cross-coupling reactions.

On the basis of previous theoretical studies of the Suzuki−Miyaura reaction,[8,13,19−28] herein we will study the mono and diphosphine routes for the coupling of PhBr and $PhB(OH)_3^-$ using $Pd(PMe_3)_2$, $Pd(PPh_3)_2$, and $Pd(PtBu_3)_2$ as catalysts. The analysis of this systems can provide information on the reason for the inefficiency of small ligand Pd complexes.

Is the diphosphine mechanism actually worse than the monophosphine one? Which factors enhance or degrade the rate of reaction? To answer these questions we will employ the energetic span model.[29−32] With this tool we can estimate the turnover frequency (**TOF**) of a reaction and the determining states that shape the kinetics of the cycle. However, to understand the reasons for the deactivation of a catalyst, we must expand the model to include more complex systems, and consider the possibility to theoretically determine the turnover number (**TON**) of a catalyst.

## TOF IN THE ENERGETIC SPAN MODEL

The TOF is the rate of reaction of a catalytic cycle, and is measured as the number of cycles ($N_{\Delta t}$) per time span ($\Delta t$) and total catalyst concentration ($[C_t]$):[1−3]

$$\mathrm{TOF} = \frac{N_{\Delta t}}{[C_t]\cdot \Delta t} \qquad (1)$$

The higher the TOF, the better the catalyst. In a recent series of papers,[29−34] a way was proposed to calculate the TOF from the energetic profile of a serial catalytic cycle: the energetic span model. This method works from the energy representation of the reaction (the E-representation), as opposed to the equivalent rate-constant representation (k-representation)[31] more typical of experimentalists (see Figure 2). It is possible to move from one representation to the other by means of Eyring's transition state theory, but the E-representation was found to be mathematically simpler and more manageable for theoreticians.

Hence, in a serial catalytic cycle with $I_j$ being the Gibbs energy of the $j^{th}$ intermediate, $T_i$ the energy of the $i$-th transition state,

Received: December 8, 2010
Revised: January 6, 2011
Published: February 22, 2011

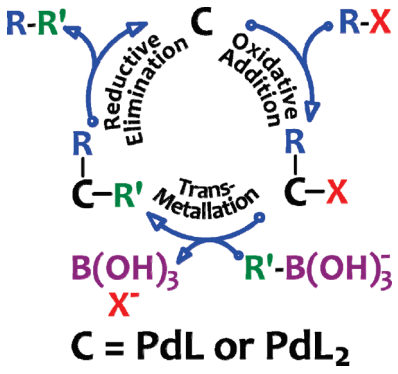


**Figure 1.** Simplified Suzuki−Miyaura reaction. First, the RX substrate is split in the oxidative addition; then, in the transmetalation step, the halide is substituted by the organic R′ group of the organoboron species; finally, in the reductive elimination the C−C bond is formed, regenerating the catalyst. The process can occur with a mono or dicoordinated Pd complex, with phosphines as the most common ligands.

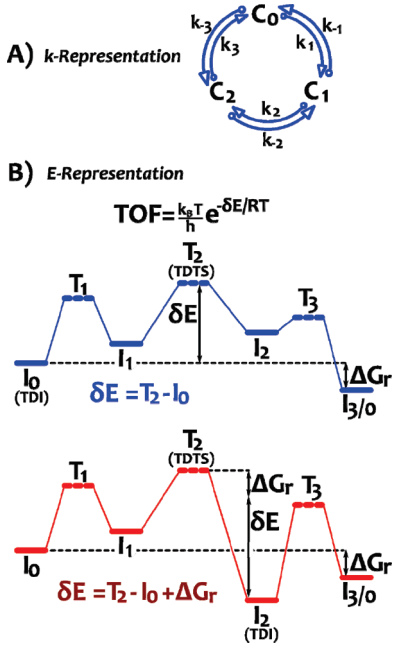


**Figure 2.** Example of a serial three-step catalytic cycle in the (A) k-representation, preferred by experimentalists, and in the (B) E-representation, favored by theoreticians. The TOF can be calculated as a function of $\delta E$, the energetic span. If the TDI comes before the TDTS, $\delta E$ is the Gibbs energy between these two states. If the TDI comes after the TDTS, we must add the reaction Gibbs energy of the full cycle[29−32].

and $\Delta G_r$ the total reaction Gibbs energy, the following TOF formula results:[29−32]

$$\mathrm{TOF} = \frac{k_B T}{h} \cdot \frac{e^{-\Delta G_r/RT} - 1}{\sum_{i,j=1}^{N} e^{(T_i - I_j - \delta G'_{i,j})/RT}} \qquad (2)$$

$$\delta G'_{i,j} = \begin{cases} \Delta G_r & \text{if} \quad i > j \\ 0 & \text{if} \quad i \leq j \end{cases}$$

If only one TS and one intermediate are determining (namely, the **TDTS** -TOF determining transition state-, and the **TDI** -TOF determining intermediate-), eq 2 can be approximated to[29−32]

$$\mathrm{TOF} = \frac{k_B T}{h} e^{-\delta E/RT} \qquad (3)$$

$$\delta E = \begin{cases} T_{TDTS} - I_{TDI} & \text{if the TDST appears after the TDI} \\ T_{TDTS} - I_{TDI} + \Delta G_r & \text{if the TDST appears before the TDI} \end{cases}$$

where $\boldsymbol{\delta E}$ is the *energetic span*,[35] that is, the apparent activation energy of the whole cycle (see Figure 2).

The TDTS and TDI can be detected as the intermediate and TS that maximize $\delta E$, according to eq 3. Alternatively, to locate the determining states we can calculate the "degree of TOF control" for transition states and intermediates ($X_{\mathrm{TOF,T}}$ and $X_{\mathrm{TOF,I}}$); the states with the highest $X_{\mathrm{TOF}}$ correspond to the TDTS and TDI.[30−32]

$$X_{\mathrm{TOF},T_i} = \frac{\sum_{j=1}^{N} e^{(T_i - I_j - \delta G'_{i,j})/RT}}{\sum_{i,j=1}^{N} e^{(T_i - I_j - \delta G'_{i,j})/RT}} \qquad (4)$$

$$X_{\mathrm{TOF},I_j} = \frac{\sum_{i=1}^{N} e^{(T_i - I_j - \delta G'_{i,j})/RT}}{\sum_{i,j=1}^{N} e^{(T_i - I_j - \delta G'_{i,j})/RT}}$$

As the $X_{\mathrm{TOF}}$ can determine the kinetic influence of all the states in the cycle, it is a useful tool to measure the validity of the energetic span approximation (eq 3). If more than one TS or one intermediate have a significant $X_{\mathrm{TOF}}$ ($\gtrsim 0.2$), eq 2 is more accurate.

It is common to observe off-cycle intermediates in equilibrium with the active species, as schematized in Figure 3. So far this "complexity" in the cycles has not been formally addressed. In these cases, if the off-cycle state ($\mathbf{C_Y}$ in Figure 3) is of lower energy compared to the species where it was originated ($\mathbf{C_X}$), it can be considered as part of the cycle by supplanting the originating molecule.[32,36] We relegate the full mathematical derivation of the off-cycle species to the appendix.

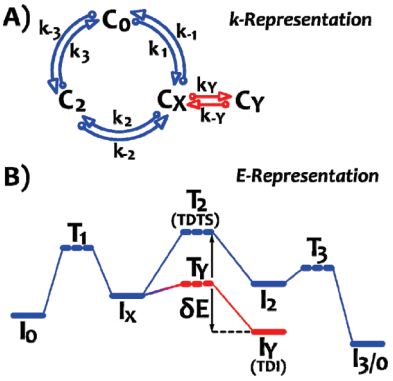


**Figure 3.** Off-cycle intermediate $\mathbf{C_Y}$ in equilibrium with the active species $\mathbf{C_X}$. If $I_Y$ (the energy of the $\mathbf{C_Y}$ intermediate) is low enough, then it can be considered the TDI (see Appendix).[32,36]

## TON IN THE ENERGETIC SPAN MODEL

The TON is the average number of cycles each catalyst molecule can provide before it gets deactivated (i.e., modified by a side reaction).[1−3] The TON is the measure of the life


dx.doi.org/10.1021/cs100129u |ACS Catal. 2011, 1, 246–253

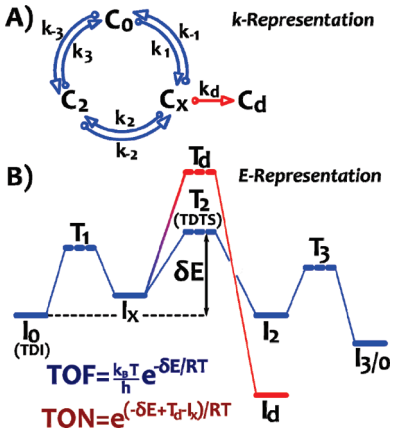


**Figure 4.** Deactivation of a catalyst by a slow irreversible side step (compare to the example of Figure 3, where the side step is in equilibrium). (A) k-representation, with a deactivation rate constant $k_d$, starting from the catalyst species $\mathbf{C}_x$ and finishing in the dead-end species $\mathbf{C}_d$. (B) Equivalent E-representation, with $T_d$ as a high Gibbs energy transition state ending in a very stable state with energy $I_d$, from where there is no return to the cycle. The TOF depends on the energetic span ($\delta E$), while the TON is affected also by the activation energy of the deactivation step.

expectancy of a catalyst, and it is sometimes more critical than the TOF, since a fast but short-lived catalyst is useless. The degradation of the catalyst occurs through an irreversible side step (with rate constant $k_d$) that slowly draws the active species to an inert species ($\mathbf{C}_d$) with very low Gibbs energy ($I_d$), as depicted in Figure 4.

The TOF is the number of turnovers that the catalyst undergoes in a certain time span ($N_{\Delta t}$), divided by the total catalyst concentration and the time interval (see eq 1). If the catalyst decays, then the TOF is a function of the time, TOF($t$). The TON, being the total number of cycles ($N$) per total catalyst concentration ($[C_t]$), can be estimated as the time integral of TOF($t$); that is, the sum of the TOF at succeeding times:

$$\mathrm{TON} = \frac{N}{[C_t]} = \int_0^\infty \mathrm{TOF}(t)\,dt \qquad (5)$$

TOF(0) is the rate of reaction at time zero, with all the catalyst still into the active cycle; it is a constant equal to an "ideal" TOF without deactivation, while TOF($t$) diminishes with a first order kinetics dependent on the deactivation rate constant $k_d$.

$$\mathrm{TOF}(t) = \mathrm{TOF}(0)\cdot e^{-k_d t} \qquad (6)$$

Inserting eq 6 into eq 5 and solving the integral, we obtain:

$$\mathrm{TON} = \mathrm{TOF}(0)\int_0^\infty e^{-k_d t}\,dt = \frac{\mathrm{TOF}(0)}{k_d} \qquad (7)$$

Applying the energetic span approximation (eq 3) and converting $k_d$ to the E-representation, we finally obtain

$$k_d = \frac{k_B T}{h} e^{-(T_d - I_x)/RT} \qquad (8)$$

$$\mathrm{TON} = e^{(-\delta E + T_d - I_x)/RT} \qquad (9)$$

From eq 9 we can see that the TON is a relation between the energetic span and the barrier for deactivation; when this barrier is equal to $\delta E$, the TON will be equal to one. Therefore, if we know the energies of the deactivation step plus the energetic span, we have a tool for understanding and possibly improving the life expectancy of a catalyst.

## THEORETICAL METHODS

The estimation of rates of reaction requires accurate theoretical data, since a small inaccuracy in the energies corresponds to an exponential error on the TOF (see eq 3). Therefore, we tested for a small model reaction several DFT functionals taking as reference CCSD(T) values. The model reaction selected was the oxidative addition of vinyl chloride on palladium mono and diphosphine complexes, including the $\eta^2$ coordination of the substrate and the transition state. This reaction resembles the electronic properties of the bigger phosphine complexes and the aryl substrate.[37,38] However, the dispersion forces of large complexes are not adequately modeled by such a small benchmark system, and DFT is known for its inability to properly assess these long-range interactions.[39,40] Hence, an important condition for the selection of the functional was a high accuracy when a dispersion correction is included (in this case we use the DFT-D3 correction by Grimme et al.[41]); in this way the accuracy observed in the small model system will not be degraded in the larger complexes. Taking into consideration accuracy (rmsd) and robustness (absence of outliers), we chose the hybrid PBE0[42] functional with the Def2-TZVPP basis set[43,44] for single point energies (see Supporting Information for complete data on the benchmark results).

For geometries, we employed the new B97D functional.[45] Being a pure GGA functional (without exact exchange), it allows applying the density fitting approximation to it, with a notable increase in the computational speed. This method makes possible geometry and frequency calculations on large complexes. As a bonus, it has a dispersion correction intrinsically embedded, and compares satisfactorily with the coupled cluster results. We used the Def2-SV(P) basis set[43,44] for geometry and frequency calculations. All the QM calculations were carried out using Gaussian 09,[46] except for the CCSD(T) benchmark, which was done with MOLPRO.[47]

Tetrahydrofuran (THF) solvation effects were included only in the single point energies, with the default polarizable continuum model of Gaussian 09 (IEFPCM). An ongoing debate questions the validity of adding thermal contributions to the energies in a solvent: the translational and rotational entropy terms are evaluated in gas-phase, which may not consider their reduction in the solvation process.[33,48−51] Ideally this should be a non-issue, since the continuum models are parametrized to experimental free energies. Recently Harvey and co-workers analyzed this assumption and concluded that, as long as the proper standard state is employed, adding gas-phase thermal corrections on solvated internal energies is the most accurate methodology,[52] and we have chosen to do so in this work. Nevertheless, we acknowledge that the solvation effect may be the source of the biggest uncertainties in the energies.

Thermal corrections are by default computed at 1 atm, which is the gas-phase standard state. However, in solution they must be converted to the standard of 1 M.[52,53] As a result, 1.89 kcal/mol must be added to every species for this conversion (equal to $RT\cdot\ln[V_l/V_g]$ at room temperature) or, equivalently, the pressure must be set to 24.45 atm.

As a summary, the theoretical method of this work consists on PBE0+D3/Def2-TZVPP(THF)//B97D/Def2-SV(P), plus thermal contribution corrected for a 1 M standard state.


dx.doi.org/10.1021/cs100129u |ACS Catal. 2011, 1, 246–253

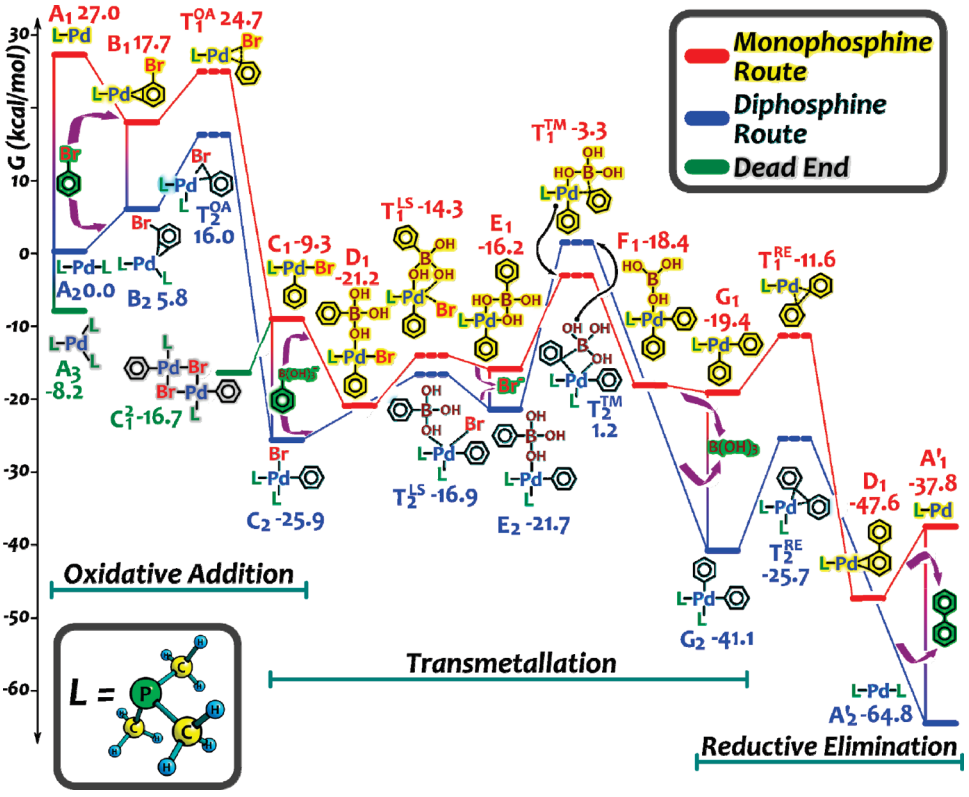


**Figure 5.** Full catalytic cycle for the monophosphine (in red) and diphosphine (in blue) routes. In green, two possible off-cycle low lying intermediates. All values are Gibbs energies in THF solvent, in kcal/mol. The vertical lines connect the species that are in equilibrium by loosing/gaining a phosphine ligand.

## RESULTS: THE CATALYTIC CYCLE

We calculated the full Suzuki−Miyaura catalytic cycle with $PMe_3$ as ligand, using PhBr and $PhB(OH)_3^-$ as the reactants to be coupled. Both the monophosphine and diphosphine routes were considered and analyzed within the energetic span model.[32] The full graph of Gibbs energies versus reaction coordinates appears in Figure 5.

**$PMe_3$: Monophosphine Route.** Let us consider first the monophosphine pathway, neglecting momentarily the diphosphine route. As the diphosphine intermediates are usually more stable than the monophosphine counterparts, this condition can only be applicable when having a stoichiometric load of ligand, or when working with bulkier phosphines. The full pathway appears in red in Figure 5.

In the monophosphine route, the TDI is located in the tetracoordinated $Pd^{II}$ complex $\mathbf{D_1}$, and the TDTS in the transmetalation transition state ($\mathbf{T_1^{TM}}$), without other states having appreciable influence ($X_{TOF}$ close to zero, see eq 4). With $\delta E$ = 17.9 kcal/mol, at standard concentrations and 25 °C, applying eq 3 yields a promising TOF of 0.5 $s^{-1}$.

The possibility of a bridged dimer was also considered (see the green intermediate $\mathbf{C_1^2}$ in Figure 5). As explained later in the Appendix, an off-cycle intermediate in equilibrium can be considered as an intermediate of the cycle itself.[32,36] Nevertheless, $\mathbf{C_1^2}$ is not low enough to result in a determining state; thus, the dimer will not affect the efficiency of the catalyst; the $\mathbf{D_1}$ state is still the TDI for the monophosphine route.

**$PMe_3$: Diphosphine Route.** Now let us consider the diphosphine route, which is somehow more realistic for small cone angle ligands (like the $PMe_3$ considered in this work). The $Pd^{II}$ center strongly prefers the tetracoordinated species, in such a way that any free phosphine will be abstracted by any tricoordinated $Pd^{II}$ complex, as depicted by the vertical lines between both routes in Figure 5. The monophosphine pathway will not be accessed, since the equivalent diphosphine molecules have lower energies.

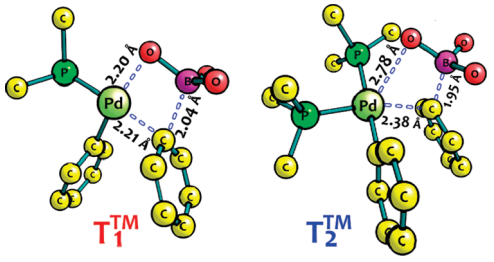


**Figure 6.** Transmetalation transition state for the monophosphine ($\mathbf{T_1^{TM}}$) and diphosphine ($\mathbf{T_2^{TM}}$) pathways. In the first, the oxygen can bond to the Pd, stabilizing the species in a planar geometry similar to the product for this step ($\mathbf{F_1}$). In the $\mathbf{T_2^{TM}}$ species, the lack of a free site forces an out-of plane geometry with higher Gibbs energy.

In this mechanism, the TDI is the $\mathbf{C_2}$ complex, right after the oxidative addition. To locate the TDTS, we must first consider that all chemical reactions will pass through the lowest accessible intermediates and transition states. The transmetalation in the diphosphine pathway ($\mathbf{T_2^{TM}}$) is higher in Gibbs energy than monophosphine equivalent TS ($\mathbf{T_1^{TM}}$), as the transfer of the phenyl group from the boron to the palladium is more accessible when having a free site (see Figure 6), and also because there is an entropy gain in the phosphine dissociation. $\mathbf{T_1^{TM}}$ is accessible from the diphosphine path just by losing one labile ligand; therefore it represents the TDTS for both pathways.


dx.doi.org/10.1021/cs100129u |ACS Catal. 2011, 1, 246–253

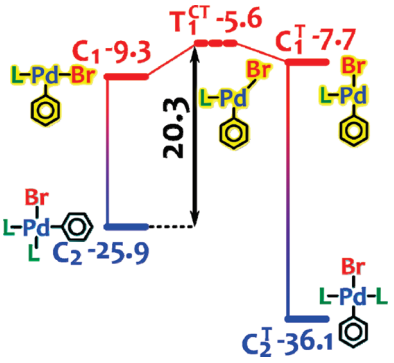


**Figure 7.** Cis−trans isomerization process ocuring after the oxidative addition step. All values are Gibbs energies in THF solvent, in kcal/mol. The trans complex remains as a low lying dead-end.

With the information of the TDI and the TDTS ($\mathbf{C_2}$ and $\mathbf{T_1^{TM}}$) we can calculate the TOF using the energetic span approximation (eq 3). At room temperature, with $\delta E = 22.6$ kcal/mol, the resulting TOF is 0.6 $h^{-1}$, substantially slower than the monophosphine route, but still a competent catalyst. Heating at 75 °C will provide the same TOF as with one phosphine at room temperature.

But with small cone angle phosphines like in this study, we must also take into account the possibility of forming the triphosphine $Pd^0$ state, depicted as $\mathbf{A_3}$ in Figure 5. This species can be included into the energetic span model as an off-cycle species in equilibrium with $\mathbf{A_2}$, as stated in the Appendix. In this case, this triphosphine complex ends up being the TDI, while the TDTS will be positioned at the oxidative addition transition state ($\mathbf{T_2^{OA}}$). The energetic span is now 24.2 kcal/mol, corresponding to a reaction rate of about 20 times slower than the cycle neglecting $\mathbf{A_3}$ (with bulkier ligands or with a very small concentration of phosphine, neglecting $\mathbf{A_3}$ would be appropriate).

**$PMe_3$: Trans Diphosphine Route.** Up to this point, we have shown that with the $PMe_3$ ligand all the pathways considered result in more or less efficient catalysis. Nevertheless, it is known that this small phosphine does not provide a proficient cycle.[13,19,20] It is also known that trans $Pd^{II}$ phosphines are more stable than their equivalent cis species[13] (the ones studied in the previous section). However, as the natural outcome of the oxidative addition is the cis isomer ($\mathbf{C_2}$ in Figure 5), there must be a cis−trans isomerization step before "falling" to the lowest-lying trans intermediates. This was previously studied,[21] and it was found that the fastest isomerization mechanism passes through the dissociation of a phosphine ligand. For the system studied herein, the energy profile of this step is shown in Figure 7.

The trans complex $\mathbf{C_2^T}$ falls to such a low Gibbs energy that it can safely be considered a dead-end, a deactivated species from where there is no return to the active cycle. As such, we can calculate the TON of the cycle according to the previous derivations. If we consider the diphosphine route to be the most probable mechanism, eq 9 will result in:

$$\mathrm{TON} = e^{(-\delta E + T_d - I_x)/RT} = e^{(-22.6 - 5.6 + 25.9)/RT} = 0.02 \quad (10)$$

From such a small theoretical TON we can say that there will be almost no reaction with this "catalyst". Unless the formation of trans complexes is obstructed, the catalyst will be deactivated faster than it can proceed with the cross-coupling cycle. The fact that a catalyst can proceed via the diphosphine mechanism will not make the catalyst completely inefficient, if it cannot reach the trans isomers.

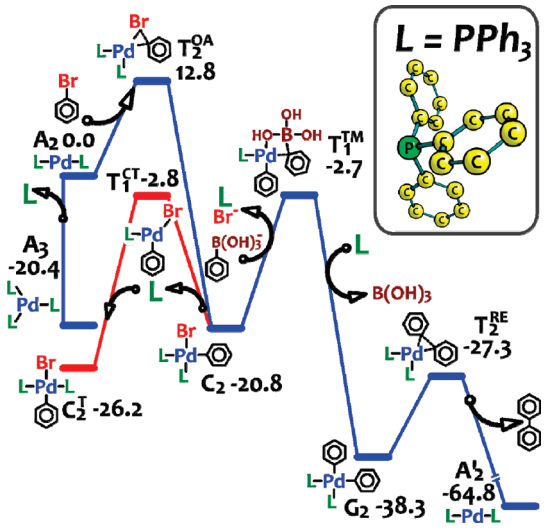


**Figure 8.** Critical states in the Pd catalyzed Suzuki−Miyaura reaction using $PPh_3$ as ligand, and their Gibbs energies in kcal/mol (the names of the states are equivalent to the $PMe_3$ system). In red the cis−trans isomerization.

There is the possibility of a slow transmetalation from the trans complex $\mathbf{C_2^T}$ (see Supporting Information). This will generate the trans equivalent to the $\mathbf{G_2}$ molecule, which not only is even lower in Gibbs energy than $\mathbf{C_2^T}$, but also cannot go through the reductive elimination to regenerate the cycle unless it isomerizes to the cis geometry through a very high energy path. One way or the other, the trans route poisons the catalyst.

In the light of this, it is not a surprise that bulky ligands that impede the tetracoordinated geometry favoring the monophosphine route are desirable. It is possible that chelating diphosphines also generates efficient catalysts for the Suzuki−Miyaura reaction by forcing the cis complexes, although the more effective monophosphine route will not be achieved.

For a full understanding of the reaction, other possible mechanisms should be included (like the anionic pathway[22−24,34,35,38,54]), but this goes beyond the scope of this work.

**$PPh_3$.** Triphenyl phosphine was one of the first active ligands for the Suzuki−Miyaura reaction.[4,5] It was quickly observed experimentally that phosphines with wider cone angle[10] provided more efficient catalysis,[1−3,13−17] and that steric effects are of greater importance than the electronic effects in cross-coupling.[18,19] In this section we will compare the bulkier $PPh_3$ ligand versus its smaller "sibling", $PMe_3$.

Both the mono and diphosphine mechanisms were considered, and similar to the $PMe_3$ system, the latter was found to provide a lower Gibbs energy pathway (see Supporting Information for all the Gibbs energies, including the monophosphine species). Evidently, to achieve the theoretically more efficient monophosphine reaction a bulkier ligand is needed. Knowing the framework of the reaction for the $PMe_3$, only the most critical states and their Gibbs energies are needed to understand the kinetics of this catalyst (see Figure 8).

Contrary to the Me based ligand, the trans $Pd^{II}$ complex $\mathbf{C_2^T}$ does not sink to a "dead-end", but to a slightly lower Gibbs energy intermediate in equilibrium with the cis isomer (see red pathway in Figure 8). From the trans $\mathbf{C_2^T}$ species, the most influential TS will be $\mathbf{T_1^{CT}}$. If we consider momentarily these two states as the TDI and TDTS, the energetic span will be 23.4 kcal/mol, with a


dx.doi.org/10.1021/cs100129u |ACS Catal. 2011, 1, 246–253

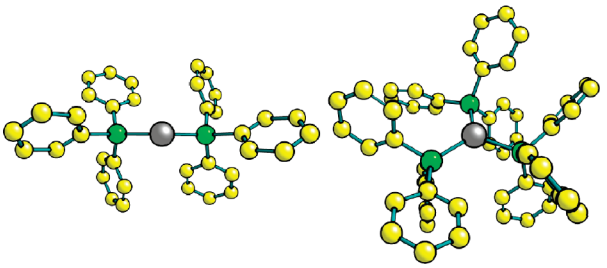

**Figure 9.** $Pd(PPh_3)_2$ and $Pd(PPh_3)_3$ complexes. In spite of the big cone angle of the ligand, the phenyl rings can penetrate into the "valleys" of the neighbor phosphine, thus making the crowded tricoordinated system a stable intermediate. However, the $\pi-\pi$ stacking energies are correctly described only when employing a dispersion correction.[41]

hypothetical TOF of 0.2 $h^{-1}$ at room temperature (see eq 3). The biggest improvement compared to the $PMe_3$ ligand is that the reaction is not fully deactivated by the generation of trans isomers, only slowed down.

In this case the formation of the triphosphine complex ($\mathbf{A_3}$) is the prime obstacle for the global reaction. As can be seen from Figure 8, the $\mathbf{A_2} + \mathbf{L} \rightarrow \mathbf{A_3}$ reaction is a highly exergonic process (20.4 kcal/mol). Considering the $\mathbf{A_3}$ intermediate as the TDI, the TDTS is the oxidative addition ($\mathbf{T_2^{OA}}$), and the energetic span will be 33.4 kcal/mol. As the reactants and products that facilitate or inhibit the cycle are the ones that are consumed or produced between the TDI and the TDTS section,[30−33] we can understand why a high concentration of ligand poisons the cycle: as a phosphine is released in the section that goes from the TDI ($\mathbf{A_3}$) to the TDTS ($\mathbf{T_2^{OA}}$), the TOF is linearly dependent (inhibited) on this concentration. The only way the $PPh_3$ system can provide an effective catalyst is by maintaining the ligand concentration strictly to a minimum, thus impeding the formation of $\mathbf{A_3}$. By the same grounds, a high concentration of the PhBr reactant will enhance the reaction, while the boronic species will not affect the TOF (as long as $\mathbf{A_3}$ is the TDI).

At this point it is appropriate to point out the importance of the dispersion correction. In the $\mathbf{A_2}/\mathbf{A_3}$ equilibrium there is a vast influence of dispersion forces on the stability of the triphosphine complex, because of the stacking of the aromatic rings (see the Supporting Information for the geometries). Neglecting the D3 correction,[41] the bonding of a third ligand will even be endergonic (3.6 kcal/mol instead of −20.4 kcal/mol when the dispersion correction is included). Most DFT methods do not include long-range dispersion interactions, and therefore may provide qualitatively wrong values for these types of reactions.

It is also important to consider the geometrical nature of this phenyl based ligand to understand the stability of the $PdL_3$ species. The $PPh_3$ cone angle is 145°,[10] but contrary to other "smoother" ligands (such as $PtBu_3$) in aromatic phosphines the effective cone angle is smaller than the tabulated one, as there are "valleys" between the phenyl rings.[34] In this way, the phenyl group of one ligand can enter into the valley of its neighbor, minimizing the steric repulsion and increasing the phenyl−phenyl stacking attraction (see Figure 9).

**$PtBu_3$.** Because of the stability and big cone angle of the *tert*-Butyl phosphine, this system has been praised as a very efficient ligand for cross-coupling catalysis.[11,12,55,56] Not only is it a bulkier ligand than the previously studied $PPh_3$ (cone angle of 182° vs 145° for the phenyl phosphine[10]), but it also lacks the "valleys" between the organic groups that made the aryl phosphines effectively smaller.[34] As

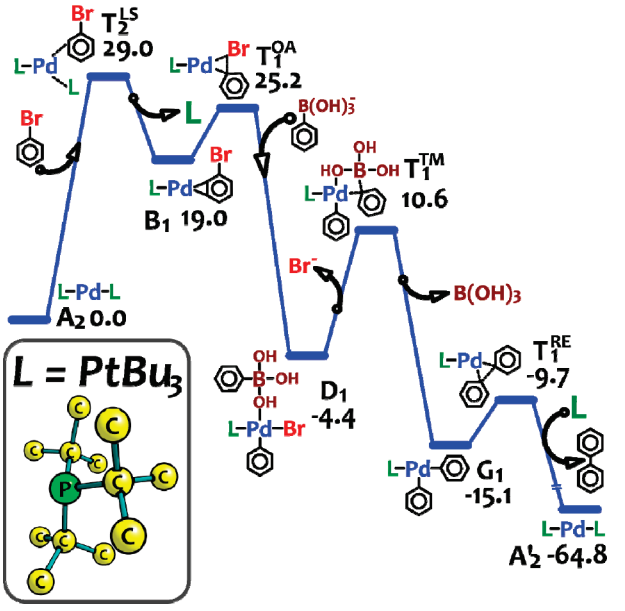


**Figure 10.** Relevant states and Gibbs energies (in kcal/mol) of the monophosphine pathway on the Suzuki−Miyaura cross-coupling with $PtBu_3$ as ligand.

a result, the diphosphine mechanism and the tricoordinated $PdL_3$ complex are greatly impeded. Indeed, we could not find stable intermediates for the square planar diphosphine $Pd^{II}$ complexes (nor the $PdL_3$ intermediate), so we only studied the monophosphine pathway, as shown in Figure 10. Interestingly, the trans diphosphines are stable complexes, although of too high Gibbs energies to be influential on the kinetics (Gibbs energy of $\mathbf{C_2^T}$: 13.2 kcal/mol). In Figure 10 we show the relevant Gibbs energy profile for this system.

The determining states are again at the beginning of the cycle. In this case the TDI is the diphosphine $Pd^0$ starting complex ($\mathbf{A_2}$), and the TDTS is the first ligand substitution, where the PhBr reactant displaces one $PtBu_3$ ligand. The resulting energetic span is 29 kcal/mol. The dissociation of one phosphine to produce the $\mathbf{A_1}$ PdL molecule (not shown in Figure 10) is also possible, with an energy of 30.0 kcal/mol. These energetic spans are significant. However, once more, the reaction will be susceptible to the concentration of the phosphine and the PhBr. A minimum quantity of the phosphine and a high concentration of PhBr will make an effective catalyst. For instance, at 100 °C, with 1 M PhBr and 0.01 M of $PtBu_3$ results in a TOF of 7 $h^{-1}$.[32] It is worth mentioning that the nature of the aryl-halide reactant will not affect the TOF significantly, as the TDTS is the phosphine substitution and the influence of the oxidative addition step is small. At room temperature and standard conditions, this reaction is estimated to be ∼1000 times faster than the $PPh_3$ system.

Neither the reductive elimination nor the oxidative addition, and not even the transmetalation, appear as determining for the $PtBu_3$ system. Thus, to further improve the performance of the catalyst, we have to provide a ligand that lowers the monophosphine $Pd^0L$ state, and at the same time lifts the diphosphine $Pd^0L_2$ complex. Theoretical studies with high cone angle ligands such as dialkylbiaryl phosphines[57] are on their way to test this hypothesis.

## CONCLUSION

Herein we studied the Suzuki−Miyaura cross-coupling reaction,[1−4] using $PMe_3$, $PPh_3$, and $PtBu_3$ as the palladium ligands.


dx.doi.org/10.1021/cs100129u |*ACS Catal.* 2011, 1, 246–253

The $PMe_3$ complex is known to be catalytically ineffective, and thus we tried to understand the reasons of this inefficiency by applying the energetic span model, as a way to improve future catalysts.

The energetic span model provides a quantitative tool to unravel the kinetics (the TOF) of a computationally studied catalytic cycle.[29−33,36,37] In this paper we expanded the model to include (I) the effect of off-cycle intermediates in equilibrium with the active cycle (see Figure 3), and (II) the effect of a deactivation step producing a dead-end (Figure 4), defining the life expectancy of a catalyst (the TON).

By inserting carefully calibrated DFT Gibbs energies into the energetic span model we reached the expected conclusion that the most efficient mechanism would be the monophosphine route, provided it does not fall into the lower energy diphosphine path. For the $PMe_3$ in the monophosphine pathway, and with phenyl bromide as the reactant, the determining intermediate (TDI) is the tetracoordinated complex $\mathbf{D_1}$, while the determining TS (TDTS) resides in the transmetalation step. The diphosphine route has lower energy states. Thus, unless we employ bulkier ligands that obstruct the formation of tetracoordinated systems, the reaction will collapse to this mechanism. At very low concentration of phosphines, we will have the determining states located in the transmetalation section ($\mathbf{C_2}$ and $\mathbf{T_1^{TM}}$ in Figure 5). But for the $PMe_3$ system and typical load of phosphines, a low lying $PdL_3$ complex ($\mathbf{A_3}$) is in fast equilibrium with the starting $PdL_2$ molecule ($\mathbf{A_2}$). This makes $\mathbf{A_3}$ the TDI, and according to eqs 3 and 4, the TDTS will now reside at the oxidative addition ($\mathbf{T_2^{OA}}$). Although much slower, the *cis* diphosphine route still provides a capable catalyst.

The death sentence of the $PMe_3$ cycle is the generation of the *trans* $PdL_2PhBr$ ($\mathbf{C_2^T}$), a low energy dead-end intermediate. The energy gap necessary to return to the active cycle is high enough to consider the cis−trans isomerization a unidirectional step, as in the example of Figure 4. Having the possibility of reaching the trans route, the TON will be too small to consider it a catalyst, even when having a theoretically reasonable TOF.

In the case of the $PPh_3$ catalyst, although the cone angle is bigger than for the previous complex, the reaction still proceeds through a diphosphine mechanism. However, the trans species are less stable than the ones of the $PMe_3$ system; thus, the isomerization process is not a dead-end in the $PPh_3$ case. The determining intermediate was found to be the $\mathbf{A_3}$ triphosphine complex, stabilized by stacking interactions between the phenyl rings. This drawback can be diminished by setting the phosphine concentration to a minimum.

The large cone angle of $PtBu_3$ permits only the monophosphine pathway, and the problematic triphosphine complex is sterically impeded. Still, the diphosphine $Pd^0L_2$ complex is a very stable species, and constitutes the TDI. Opposed to the previous systems, the oxidative addition is less critical, typical of a monophosphine mechanism. The first phosphine dissociation is the determining transition state; thus, again this reaction is affected by the concentration of this ligand. The $PtBu_3$ cycle is expected to be a thousand times faster than the $PPh_3$ at room temperature.

Following these directions, in subsequent works we will analyze through the energetic span model the efficiency of complexes bearing more complex phosphines.

## APENDIX: MATHEMATICAL DERIVATION OF OFF-CYCLE INTERMEDIATES IN EQUILIBRIUM

Frequently in catalytic cycles, an off-cycle intermediate occurs in equilibrium with the simple cycle. When this deviation from the pathway results in a low-lying intermediate, its influence cannot be neglected, as it can lead to a new kind of TDI. Figure 3A shows the k-representation of a three steps cycle with an out of the cycle intermediate $\mathbf{C_Y}$ generated from an active species $\mathbf{C_X}$. We can express the TOF using Cramer's rule as follows:[30]

$$\mathrm{TOF} = \frac{k_i \det \hat{A}_{i-1} - k_{-i} \det \hat{A}_i}{\det \hat{A}} \tag{a1}$$

For the definition of the $\hat{A}$ matrix see ref 30. When having an off-cycle state, $\hat{A}$ will have one additional row and column compared to the serial cycle case. Defining $\hat{A}^S$ as the matrix of the serial system (without $\mathbf{C_Y}$), and for the sake of algebraic simplicity considering $\mathbf{C_X}$ being the last state of the cycle, we can write:

$$\hat{A} = \begin{pmatrix} \cdots & 0 & k_Y & k_{-Y} \\ & & & 0 \\ & \hat{A}^S & & \vdots \\ & & & 1 \end{pmatrix} \tag{a2}$$

Resolving the determinant results in

$$\det \hat{A} = k_{-Y} \det \hat{A}^S + k_Y \det \hat{A}_X^S \tag{a3}$$

$$\det \hat{A}_i = -k_{-Y} \det \hat{A}_i^S \tag{a4}$$

resulting in a TOF of

$$\mathrm{TOF} = \frac{e^{\sum_{i=1}^{N}(I_i - T_i)} \cdot (e^{-\Delta G_r} - 1)}{\det \hat{A}^S - \frac{k_Y}{k_{-Y}} \det \hat{A}_X^S} \tag{a5}$$

with

$$\det \hat{A}^S = e^{\sum_{i=1}^{N}(I_i - T_i)} \cdot \sum_{l,m=1}^{N} (T_l - I_m - \delta G'_{l,m}) \tag{a6}$$

$$\det \hat{A}_X^S = e^{\sum_{i=1}^{N}(I_i - T_i)} \cdot \sum_{l=1}^{N} (T_l - I_X - \delta G'_{l,m}) \tag{a7}$$

$$\frac{k_Y}{k_{-Y}} = e^{I_X - T_Y} \tag{a8}$$

Inserting eqs a6, a7 and a8 into a5 the TOF can finally be expressed as

$$\mathrm{TOF} = \frac{e^{-\Delta G_r} - 1}{\left( \sum_{l,m=1}^{N} e^{T_l - I_m - \delta G'_{l,m}} \right) + \left( e^{-I_Y} \cdot \sum_{l=1}^{N} e^{T_l - \delta G'_{l,X}} \right)} \tag{a9}$$

Equation a9 is essentially equal to the TOF equation for serial catalytic cycles (eq 2), but it adds a series of terms in the denominator where it combines the energy of intermediate $\mathbf{C_Y}$ with all the transition states energies. Note that there is no reference to the TS that leads from $\mathbf{C_X}$ to $\mathbf{C_Y}$, since we consider a steady state regime; $\mathbf{C_X}$ and $\mathbf{C_Y}$ must be in fast equilibrium for this to occur.


dx.doi.org/10.1021/cs100129u |*ACS Catal.* 2011, 1, 246–253

In the energetic span approximation, we can consider $I_Y$ as another intermediate energy coming from $I_X$. So, if $\mathbf{C_Y}$ results the TDI (as exemplified in Figure 3), then

$$\delta E = \begin{cases} T_{TDTS} - I_Y & \text{if the TDST appears after } C_X \\ T_{TDTS} - I_Y + \Delta G_r & \text{if the TDST appears before } C_X \end{cases} \quad \text{(a10)}$$

From this expression the rule of thumb is as follows: if $I_Y$ is lower than $I_X$, change state $\mathbf{C_X}$ by state $\mathbf{C_Y}$ and use the energetic span model in its simple form. In the opposite case, one can safely neglect the off-cycle species.[32,36]

## ■ ASSOCIATED CONTENT

**Supporting Information.** Benchmark energies, geometries of all species and Gibbs energies for the transmetalation of the trans route. This material is available free of charge via the Internet at http://pubs.acs.org.

## ■ AUTHOR INFORMATION

**Corresponding Author**
*E-mail: sebastian.kozuch@weizmann.ac.il.

## ■ ACKNOWLEDGMENT

We thank Prof. Jeremy Harvey for valuable discussions and comments. S.K. is a Koshland Postdoctoral Fellow. This research was supported by the Weizmann Institute AERI (Alternative Energy Research Initiative), by the Lise Meitner-Minerva Center for Computational Quantum Chemistry, and by the Helen and Martin Kimmel Center for Molecular Design.

## ■ REFERENCES

(1) van Leeuwen, P. W. N. M. *Homogeneous catalysis: understanding the art*; Kluwer Academic Publishers: Dordrecht; Boston, 2004.
(2) Astruc, D. *Organometallic chemistry and catalysis*; Springer: Berlin; New York, 2007.
(3) Hartwig, J. *Organotransition metal chemistry: from bonding to catalysis*; University Science Books: Sausalito, CA, 2010.
(4) Miyaura, N.; Suzuki, A. *Chem. Rev.* **1995**, *95*, 2457–2483.
(5) Pigge, F. *Synthesis* **2010**, *2010*, 1745–1762.
(6) Wu, X.; Anbarasan, P.; Neumann, H.; Beller, M. *Angew. Chem., Int. Ed.* **2010**, *49*, 9047–9050.
(7) Kotha, S.; Lahiri, K.; Kashinath, D. *Tetrahedron* **2002**, *58*, 9633–9695.
(8) Braga, A. A.; Morgon, N. H.; Ujaque, G.; Lledós, A.; Maseras, F. *J. Organomet. Chem.* **2006**, *691*, 4459–4466.
(9) Braga, A. A. C.; Morgon, N. H.; Ujaque, G.; Maseras, F. *J. Am. Chem. Soc.* **2005**, *127*, 9298–9307.
(10) Tolman, C. A. *Chem. Rev.* **1977**, *77*, 313–348.
(11) Littke, A. F.; Fu, G. C. *J. Am. Chem. Soc.* **2001**, *123*, 6989–7000.
(12) Littke, A. F.; Fu, G. C. *J. Org. Chem.* **1999**, *64*, 10–11.
(13) Ariafard, A.; Yates, B. F. *J. Am. Chem. Soc.* **2009**, *131*, 13981–13991.
(14) Fleckenstein, C. A.; Plenio, H. *Chem. Soc. Rev.* **2010**, *39*, 694.
(15) Christmann, U.; Vilar, R. *Angew. Chem., Int. Ed.* **2005**, *44*, 366–374.
(16) Molander, G.; Canturk, B. *Angew. Chem., Int. Ed.* **2009**, *48*, 9240–9261.
(17) Littke, A. F.; Fu, G. C. *Angew. Chem., Int. Ed.* **2002**, *41*, 4176–4211.
(18) Barder, T. E.; Walker, S. D.; Martinelli, J. R.; Buchwald, S. L. *J. Am. Chem. Soc.* **2005**, *127*, 4685–4696.
(19) Moncho, S.; Ujaque, G.; Lledós, A.; Espinet, P. *Chem.—Eur. J.* **2008**, *14*, 8986–8994.
(20) Jover, J.; Fey, N.; Purdie, M.; Lloyd-Jones, G. C.; Harvey, J. N. *J. Mol. Catal. A: Chem.* **2010**, *324*, 39–47.
(21) Braga, A. A. C.; Ujaque, G.; Maseras, F. *Organometallics* **2006**, *25*, 3647–3658.
(22) Goossen, L. J.; Koley, D.; Hermann, H. L.; Thiel, W. *J. Am. Chem. Soc.* **2005**, *127*, 11102–11114.
(23) Goossen, L. J.; Koley, D.; Hermann, H. L.; Thiel, W. *Organometallics* **2005**, *24*, 2398–2410.
(24) Goossen, L. J.; Koley, D.; Hermann, H. L.; Thiel, W. *Organometallics* **2006**, *25*, 54–67.
(25) Sicre, C.; Braga, A. A. C.; Maseras, F.; Cid, M. M. *Tetrahedron* **2008**, *64*, 7437–7443.
(26) Huang, Y.; Weng, C.; Hong, F. *Chem.—Eur. J.* **2008**, *14*, 4426–4434.
(27) Li, Z.; Fu, Y.; Guo, Q.; Liu, L. *Organometallics* **2008**, *27*, 4043–4049.
(28) Schoenebeck, F.; Houk, K. N. *J. Am. Chem. Soc.* **2010**, *132*, 2496–2497.
(29) Kozuch, S.; Shaik, S. *J. Am. Chem. Soc.* **2006**, *128*, 3355–3365.
(30) Kozuch, S.; Shaik, S. *J. Phys. Chem. A* **2008**, *112*, 6032–6041.
(31) Kozuch, S.; Shaik, S. *Acc. Chem. Res.* **2010**, ASAP.
(32) Uhe, A.; Kozuch, S.; Shaik, S. *J. Comput. Chem.* **2010**, ASAP.
(33) Kozuch, S.; Lee, S. E.; Shaik, S. *Organometallics* **2009**, *28*, 1303–1308.
(34) Kozuch, S.; Shaik, S. *J. Mol. Catal. A* **2010**, *324*, 120–126.
(35) Amatore, C.; Jutand, A. *J. Organomet. Chem.* **1999**, *576*, 254–278.
(36) Meir, R.; Kozuch, S.; Uhe, A.; Shaik, S. *Chem.—Eur. J.* **2010** accepted.
(37) Carvajal, M. A.; Kozuch, S.; Shaik, S. *Organometallics* **2009**, *28*, 3656–3665.
(38) Kozuch, S.; Shaik, S.; Jutand, A.; Amatore, C. *Chem.—Eur. J.* **2004**, *10*, 3072–3080.
(39) Sieffert, N.; Bühl, M. *Inorg. Chem.* **2009**, *48*, 4622–4624.
(40) McMullin, C. L.; Jover, J.; Harvey, J. N.; Fey, N. *Dalton Trans* **2010**, *39*, 10833–10836.
(41) Grimme, S.; Antony, J.; Ehrlich, S.; Krieg, H. *J. Chem. Phys.* **2010**, *132*, 154104.
(42) Adamo, C.; Barone, V. *J. Chem. Phys.* **1999**, *110*, 6158.
(43) Weigend, F.; Ahlrichs, R. *Phys. Chem. Chem. Phys.* **2005**, *7*, 3297.
(44) Schäfer, A.; Huber, C.; Ahlrichs, R. *J. Chem. Phys.* **1994**, *100*, 5829.
(45) Grimme, S. *J. Comput. Chem.* **2006**, *27*, 1787–1799.
(46) Frisch, M. J. et al. *Gaussian 09*, Rev. A02; Gaussian, Inc.: Wallingford, CT, 2009.
(47) Werner, H. J. et al.; *MOLPRO*, Version 2009.1; http://www.molpro.net, 2009.
(48) Dub, P. A.; Poli, R. *J. Mol. Catal. A: Chem.* **2010**, *324*, 89–96.
(49) Ardura, D.; López, R.; Sordo, T. L. *J. Phys. Chem. B* **2005**, *109*, 23618–23623.
(50) Leung, B. O.; Reid, D. L.; Armstrong, D. A.; Rauk, A. *J. Phys. Chem. A* **2004**, *108*, 2720–2725.
(51) Cooper, J.; Ziegler, T. *Inorg. Chem.* **2002**, *41*, 6614–6622.
(52) Harvey, J. N. *Faraday Discuss.* **2010**, *145*, 487.
(53) General, I. J. *J. Chem. Theory Comput.* **2010**, *6*, 2520–2524.
(54) Amatore, C.; Jutand, A.; Lemaitre, F.; Ricard, J. L.; Kozuch, S.; Shaik, S. *J. Organomet. Chem.* **2004**, *689*, 3728–3734.
(55) Fu, G. C. *Acc. Chem. Res.* **2008**, *41*, 1555–1564.
(56) Littke, A. F.; Fu, G. C. *Angew. Chem., Int. Ed.* **1998**, *37*, 3387–3388.
(57) Martin, R.; Buchwald, S. L. *Acc. Chem. Res.* **2008**, *41*, 1461–1473.